Inelastic He-atom scattering from the MgO(001) surface

Jinhe Cui, David R. Jung, and Daniel R. Frankl

Department of Physics, The Pennsylvania State University, University Park, Pennsylvania 16802

(Received 30 April 1990)

Dispersion curves of Rayleigh phonons on an *in situ* cleaved, room-temperature surface of MgO(001) are determined by time-of-flight measurements of inelastically scattered He atoms. Along both the $\bar{\Gamma}\bar{X}$ and $\bar{\Gamma}\bar{M}$ directions, the measured phonon frequencies agree fairly well with a shell-model calculation for an unrelaxed MgO(001) surface.

Since the first successful measurement of the full dispersion curve of the Rayleigh wave on a LiF(100) surface,[1,2] inelastic He-atom scattering has become a powerful technique to study surface phonons. To date, a number of ionic crystals and a few semiconductor and metal surfaces have been studied by this method.[3-5] The measurements on ionic crystals indicate that the surface-localized vibrational modes, particularly the Rayleigh mode, can be described fairly well by a shell-model calculation on a thin slab.[6] One exception was found in the case of LiF, where the vibrational frequency of the Rayleigh wave at the zone boundary was predicted to be 11% higher than observed.[1,2] The discrepancy was variously attributed to a change of anion polarizability at the surface,[7] surface-charge transfer, and a change of transverse force constant at the surface.[8]

From the theoretical point of view, the surface vibrational modes on MgO and LiF share several common features owing, in part, to the fact that both crystals have a cubic anisotropy parameter η $[\eta = c_{44}/(c_{11} - c_{22})]$ greater than 1.[6] Along the $\bar{\Gamma}\bar{M}$ direction ($\langle 100 \rangle$ azimuth), the lowest-frequency acoustical model (designated S_1) is the Rayleigh mode (i.e., polarized in the sagittal plane), lying below the bulk band edge. Along the $\bar{\Gamma}\bar{X}$ direction ($\langle 110 \rangle$ azimuth), however, the S_1 mode is predicted to have a shear horizontal polarization, and thus cannot couple to in-plane-scattered He atoms in one-phonon interactions.[9] The Rayleigh mode is predicted to lie in the bulk band.

The lattice dynamics of the MgO surface is interesting also because of the possibility of large surface-charge redistribution. The ionicity of the oxygen ion in bulk MgO is O^{2-}, compared with O^- type ionicity in molecular MgO.[10] In bulk MgO, each O^{2-} ion has six neighbors while it only has five neighbors at the surface. Therefore the ionicity of the oxygen ion at the surface is expected to be intermediate between those of bulk and molecular MgO. The experimental observation of relatively small corrugation of the surface-charge density is thought to corroborate this idea.[11,12] As indicated in the theoretical lattice-dynamics study of LiF,[7,8] such charge transfer should cause changes in the frequency of surface phonons, and therefore can be detected by inelastic He-atom scattering.

Prior to our work, the $\langle 100 \rangle$ azimuth of the MgO(001)

surface was studied by inelastic He scattering only on an air-cleaved sample.[13] In this measurement, single-phonon features were observed only near the zone center ($Q \leq 0.5$ Å^{-1}) and only when the surface was heated to 750 K. In this paper we report our results of time-of-flight (TOF) inelastic He-atom scattering measurements from *in situ* cleaved MgO(001) surfaces. Owing to the better surface quality which results from the *in situ* cleaving process,[12,14] we are able to observe single-phonon excitation of Rayleigh waves along both $\langle 100 \rangle$ and $\langle 110 \rangle$ azimuths out to the regions near the zone boundary.

Most parts of our apparatus have been described before.[15,16] The He beam is produced by expanding high-pressure (300–450 psi) He gas through a nozzle cooled by liquid nitrogen. Nozzle sizes of 5 and 7.5 μm have been used, giving a velocity spread of the beam of 1%. The beam is chopped by a 2-in. diam. rim-type chopper (Ref. 16) which has two equally spaced slots 0.02-in. wide. At the rotation frequency of 120 Hz, the pulse width determined by the TOF spectrum of a specular reflection from the MgO surface is about 24 μsec, which corresponds to an energy resolution of 1 meV. The detector is a sensitive low-resolution magnetic mass spectrometer copied from the design of Lilienkamp and Toennies.[17] The angle between the detector axis and the incident beam is fixed at 90.2°. The data are collected with a multichannel analyzer (Nicolet No. 1170) with the channel width set at 6 μsec. TOF spectra were obtained by averaging the signal in each channel for 0.5–2.0 $\times 10^6$ cycles, so that the recording time for each spectrum ranged from 1 to 4 h. The detector chamber is pumped by a 360 l/s turbomolecular pump backed by a 50 l/s turbomolecular pump, with a Titanium sublimation pump in parallel. The base pressure in the detector chamber was about 3×10^{-10} Torr. The scattering chamber is pumped by a 600 l/s cryopump and the base pressure was about 5×10^{-10} Torr. The flight tube between the scattering and detector chambers consists of three differential pumping stages separated by apertures of 3 to 6 mm diameter, each pumped by a 50 l/s turbomolecular pump. The distance between the middle of the 2-cm-long ionization cage of the detector and the sample is about 99.6±0.1 cm. The angular acceptance of the detector is about 0.2° and width of the incident beam is about 0.1°.

At the nozzle temperature of 80 K, the wave vector of

            ©1990 The American Physical Society

the incident beam (k_i) is about 5.77 Å^{-1} as determined by measuring the angular positions of diffraction beams. The variation of k_i from day to day was observed to be about ± 0.015 Å^{-1}. The MgO crystal (Spicer Ltd., London, England) was cleaved *in situ* and kept at room temperature. To check the quality of the freshly cleaved surface, the ratio of the specular intensity at 45° to the incident intensity was measured using a movable detector inside the scattering chamber.[12,14,15] The ratio was typically 8–12 %. After the cleave, the surface quality was found to degrade gradually as judged by the intensities of specular and diffraction beams. Therefore a new cleave was usually made after about 5–6 days.

The principal azimuthal directions of the surface were determined by maximizing the intensities of diffraction beams. Figure 1 shows two angular scans taken along the $\langle 100 \rangle$ and $\langle 110 \rangle$ azimuths. These scans were made with an unchopped He beam, and the incident polar angle θ_i was changed in increments of 0.05° in the vicinity of specular and diffraction beams and 0.2° otherwise. As one can see from the lower traces of Fig. 1, the intensities of diffraction beams along both azimuths are about 10–25 % of that of the specular beams. Furthermore the ratio of the diffraction to the specular intensity does not show a large difference from one azimuth to the other, in contrast to some alkali halides such as LiF, NaF,[2] and KBr.[3] These observations can be understood based on the hard corrugated surface model and the relatively small surface corrugation on the MgO(001) surface.[11,12]

Along the $\langle 100 \rangle$ azimuth, the full width at half maximum (FWHM) of the ($\bar{1}0$), (00), and (10) beams is 0.26°, 0.11°, and 0.19°, respectively, while along the $\langle 110 \rangle$ azimuth, the FWHM of the ($\bar{1}\bar{1}$), (00), and (11) beams is 0.20°, 0.10°, and 0.13°, respectively. These widths are consistent with the velocity spread of the beam. The upper traces in Figs. 1(a) and 1(b) clearly show the presence of inelastic- as well as incoherent elastic-scattered He atoms. Some of the maxima and minima observed between the specular and diffraction beams can be attributed to the surface-phonon-assisted bound-state resonances.

In Fig. 2, two sample TOF spectra, one taken along $\langle 100 \rangle$ and the other along $\langle 110 \rangle$ azimuths, are presented. The peaks labeled E are due to diffuse elastic scattering from surface defects such as steps and impurities, as has been commonly observed on other surfaces including alkali halides, metals, and semiconductors. We observed this feature at all incident angles studied ranging from 26° to 71°. The strongest diffuse elastic scattering was found at angles near the specular and diffraction peaks along the $\langle 100 \rangle$ direction. In these regions, the intensity of the

FIG. 1. Angular distribution of scattered He taken along (a) $\langle 100 \rangle$ and (b) $\langle 110 \rangle$ azimuths of an *in situ* cleaved MgO(001) surface. The data are presented on two scales that are different by a factor of 2500 to show all the features of interest.
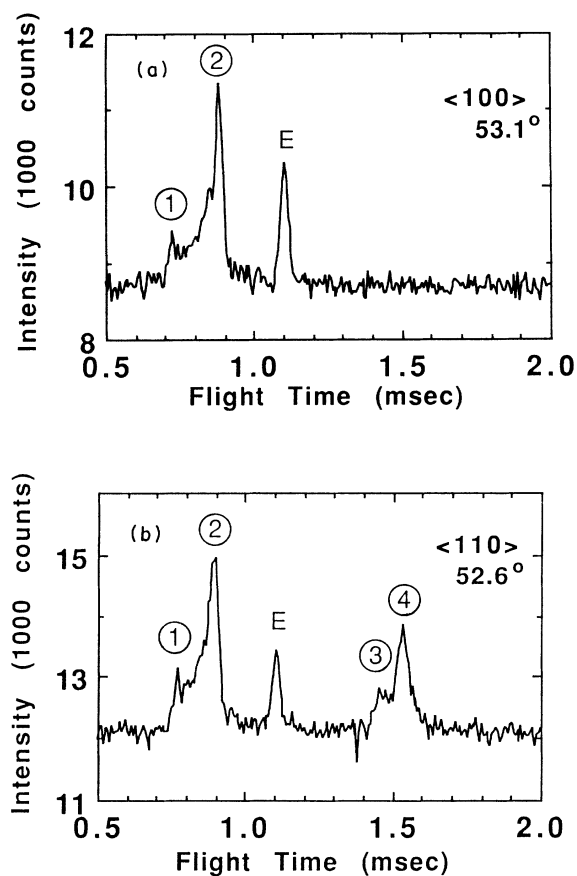
FIG. 2. TOF spectra of 17.4-meV He atoms scattered from a MgO(001) surface. The incident angle θ_i is (a) 53.1° and (b) 52.6°. The flight time is from sample to detector, and the channel width is 6 μsec. The letter E indicates a diffuse elastic peak. 1 and 2 refer to the annihilation, 3 and 4 to the creation phonon peaks, respectively. The typical counting time for each TOF spectrum ranges from 1 to 4 h corresponding to $(0.5-2.0) \times 10^6$ cycles signal averaging.

diffuse elastic scattering can be more than 5 times larger than that of the strongest inelastic features even at incident angles as much as 1.5° away from the elastic beams. This factor is much larger than that along the ⟨110⟩ direction and is also much larger than that observed on the alkali-metal halides such as LiF, NaF, KCl,[2] KBr, and RbBr.[3] At angles between specular and diffraction peaks, the diffuse elastic scattering becomes much less intense and varies slowly with the incident angle. However, even in this region, its intensity is still 50–100 % larger along ⟨100⟩ than along ⟨110⟩. These observations suggest the presence of a large number of atomic steps preferentially oriented along the ⟨100⟩ directions on the MgO(001) surface.

The other sharp peaks (labeled by numbers) in Fig. 2 are caused by the excitation of surface and bulk phonons in single-phonon processes. Those (peaks 1 and 2) on the left side of the elastic peak are due to phonon annihilation events and those (peaks 3 and 4) on the right side are due to phonon creation events. In addition, there is also some inelastic intensity between two annihilation peaks. This, however, can be attributed to the excitation of bulk phonons. At the angles near the positions of diffraction beams, we also observed "spurious" peaks due to the elas-

tic tail of diffraction beams. These peaks were not observed at angles more than 5° away from that of diffraction beams, and therefore they do not appear in the spectra presented in Fig. 2.

The phonon energy $\hbar\omega$ and wave vector $\mathbf{Q}$ are determined via the conservation of energy and parallel crystal momentum,

$$\hbar\omega = (\hbar^2/2m)(k_f^2 - k_i^2) \qquad (1)$$

and

$$\mathbf{K}_f - \mathbf{K}_i = \mathbf{G} + \mathbf{Q} , \qquad (2)$$

where $\mathbf{K}_f$ and $\mathbf{K}_i$ are the surface projections of the final and incident wave vectors $\mathbf{k}_f$ and $\mathbf{k}_i$, respectively, and $\mathbf{G}$ is a surface reciprocal-lattice vector. The resulting values of phonon energy and wave vector are plotted in repeated surface Brillouin zones for the ⟨100⟩ [Fig. 3(a)] and ⟨110⟩ [Fig. 3(b)] directions, respectively. The solid lines in both Figs. 3(a) and 3(b) are the calculated dispersion curve of the Rayleigh wave for an unrelaxed MgO(001) surface.[6] In Fig. 3(b), the calculated dispersion curve of a shear horizontal (SH) mode is also shown by a dashed line for comparison. According to the shell-model calculation of Chen et al.,[6] the Rayleigh mode is the lowest-frequency vibrational mode along ⟨100⟩ while the SH mode is the lowest-frequency mode along ⟨110⟩. Most of our data agree fairly well with the calculated dispersion curve of the Rayleigh mode along the both azimuths. This is consistent with the fact that in-plane-scattered He atoms do not couple with the SH mode. Some of the data, such as peak 4 in Fig. 3(b), do not coincide with the dispersion curve of the Rayleigh model. These points are located near the reciprocal-lattice vectors $(\bar{1}\,\bar{1})$ or $(\bar{1}0)$. The analysis of the kinematics of these features indicates that they are caused by the resonance-enhanced excitation of bulk phonons. The good agreement between the theory and the experiment suggests that the lattice dynamics of MgO(001) can be described quite well by the shell-model calculation for the unrelaxed surface. It also suggests that surface relaxation, surface rumpling, and the surface charge redistribution on the cleaved MgO(001) surface is small. Our result is consistent with claims based on low-energy electron diffraction[18] and a self-consistent-field calculation[19] that the surface of MgO is nearly identical to a simple truncation of the bulk.

In summary, we measured the Rayleigh wave dispersion on an in situ cleaved MgO(001) surface by inelastic He atom scattering. Our results agree with the shell-model calculation for an unrelaxed MgO(001) surface.[6] We also observed very large diffuse elastic scattering, which is attributed to the presence of large density of steps on the cleaved MgO(001) surface.
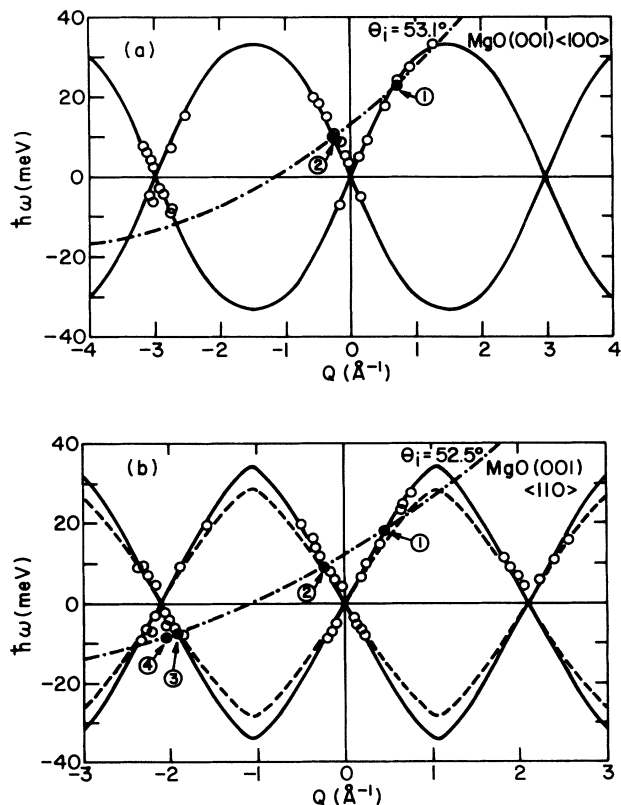
FIG. 3. Repeated zone plot of the measured surface phonon energies and wave vectors. The measurements were taken along the principal symmetry directions (a) ⟨100⟩ and (b) ⟨110⟩. The solid and dashed lines are the Rayleigh and SH surface modes calculated for an unrelaxed MgO(001) surface (Ref. 6). The dashed-dotted lines are the scan curves at $\theta_i = 53.1°$ (along ⟨100⟩) and $\theta = 52.6°$ (along ⟨110⟩). The single-phonon peaks (solid circles) observed in Fig. 2 are indicated by the same labels used in Fig. 2.

[1]G. Brusdeylins, R. B. Doak, and J. P. Toennies, Phys. Rev. Lett. **46**, 437 (1981).

[2]G. Brusdeylins, R. B. Doak, and J. P. Toennies, Phys. Rev. B **27**, 3662 (1983).

[3]J. P. Toennies, Phys. Scr. T **19**, 39 (1987).

[4]P. Zeppenfeld, K. Kern, R. David, K. Kuhnke, and G. Comsa, Phys. Rev. B **38**, 12 329 (1988).

[5]G. Chern, J. G. Skofronick, W. P. Brug, and S. A. Safron, Phys. Rev. B **39**, 12 828 (1989); **39**, 12 838 (1989).

[6]T. S. Chen, F. W. de Wette, and G. P. Alldrege, Phys. Rev. B **15**, 1167 (1977).

[7]G. Benedek, G. P. Brivio, L. Miglio, and V. R. Velasro, Phys. Rev. B **26**, 497 (1982).

[8]W. Kress, F. W. de Wette, A. D. Kulkarni, and U. Schroder, Phys. Rev. B **35**, 2467 (1987).

[9]V. Celli and D. Eichenauer, in *Proceedings of the 2nd International Conference on Phonon Physics, Budapest, 1985,* edited by J. Kollár, N. Kroó, N. Menyhárd, and T. Siklós (World Scientific, Singapore, 1985), p. 612.

[10]A. J. Martin and H. Bilz, Phys. Rev. B **19**, 6593 (1979).

[11]K. H. Rieder, Surf. Sci. **118**, 57 (1982).

[12]D. R. Jung, M. Mahgerefteh, and D. R. Frankl, Phys. Rev. B **39**, 11 164 (1989).

[13]G. Brusdeylins, R. Bruce Doak, J. G. Skofronick, and J. P. Toennies, Surf. Sci. **128**, 191 (1983).

[14]M. Mahgerefteh, D. R. Jung, and D. R. Frankl, Phys. Rev. B **39**, 3900 (1989).

[15]S. Chung, A. Kara, J. Z. Larese, W. Y. Leung, and D. R. Frankl, Phys. Rev. B **35**, 4870 (1987).

[16]B. D. Weaver and D. R. Frankl, Rev. Sci. Instrum. **59**, 92 (1988).

[17]J. P. Toennies, private communication; Gerhard Lilienkamp, Ph.D. thesis, Max-Planck-Institut für Strömungsforschung, 1981 (unpublished).

[18]M. Prutton, J. A. Walker, M. R. Welton-Cook, R. C. Felton, and J. A. Ramsey, Surf. Sci. **89**, 95 (1979); T. Urano, T. Kanaji, and M. Kaburagi, *ibid.* **134**, 109 (1983).

[19]P. W. Fowler and P. Tole, Surf. Sci. **197**, 457 (1988).